Form Approved
OBM No. 0704-0188

1. Agency Use Only *(Leave blank).*

2. Report Date. February 1994

3. Report Type and Dates Covered. Final - Journal Article

4. Title and Subtitle.
Assimilation of Altimeter Data in a Two-Layer Primitive Equation Model of the Gulf Stream

5. Funding Numbers.
Program Element No. 0602435N
Project No. RM35G93
Task No. 201
Accession No. DN251050
Work Unit No. 13231D

6. Author(s).
Ole Martin Smedstad* and Daniel N. Fox

7. Performing Organization Name(s) and Address(es).
Naval Research Laboratory
Ocean Dynamics and Prediction Branch
Stennis Space Center, MS 39529-5004

8. Performing Organization Report Number.
NRL/JA/7323--92-0001

9. Sponsoring/Monitoring Agency Name(s) and Address(es).
Office of Naval Research
800 N. Quincy Street
Arlington, VA 22217

10. Sponsoring/Monitoring Agency Report Number.
NRL/JA/7323--92-0001

11. Supplementary Notes.
Published in Journal of Physical Oceanography.
*Planning Systems Incorporated, Slidell, LA

12a. Distribution/Availability Statement.
Approved for public release; distribution is unlimited.

12b. Distribution Code.

13. Abstract *(Maximum 200 words).*

A two-layer finite depth, primitive equation model of the Gulf Stream region is used to study the effect of updating the model with simulated altimeter data as observations. In this study both a complete field of sea surface height (SSH) and SSH sampled along satellite tracks are used as "observations." A simulated 17-day repeat orbit corresponding to the Geosat-ERM and a 10-day repeat period corresponding to Topex/Poseidon are used. Satellite observations give only information about the sea surface height but previous studies have shown that it is important to transfer the surface information to the lower layer as fast as possible in order for the model to have a realistic evolution. A statistical inference technique is therefore used to update the lower-layer pressure field. The velocity fields in both layers are updated using a geostrophic correction calculated from the change in the pressure fields. It is shown that updating the velocities is important for the assimilation to be successful.

14. Subject Terms.
Ocean models, ocean forecasting, fronts, air-sea interaction

15. Number of Pages. 21

16. Price Code.

17. Security Classification of Report.	18. Security Classification of This Page.	19. Security Classification of Abstract.	20. Limitation of Abstract.
Unclassified	Unclassified	Unclassified	SAR

Reprinted from JOURNAL OF PHYSICAL OCEANOGRAPHY, Vol. 24, No. 2, February 1994
American Meteorological Society

Assimilation of Altimeter Data in a Two-Layer Primitive Equation Model of the Gulf Stream*

OLE MARTIN SMEDSTAD

Planning Systems Incorporated, Slidell, Louisiana

DANIEL N. FOX

Naval Research Laboratory, Stennis Space Center, Mississippi

(Manuscript received 12 October 1992, in final form 3 May 1993)

ABSTRACT

A two-layer finite depth, primitive equation model of the Gulf Stream region is used to study the effect of updating the model with simulated altimeter data as observations. In this study both a complete field of sea surface height (SSH) and SSH sampled along satellite tracks are used as "observations." A simulated 17-day repeat orbit corresponding to the Geosat-ERM and a 10-day repeat period corresponding to Topex/Poseidon are used. Satellite observations give only information about the sea surface height but previous studies have shown that it is important to transfer the surface information to the lower layer as fast as possible in order for the model to have a realistic evolution. A statistical inference technique is therefore used to update the lower-layer pressure field. The velocity fields in both layers are updated using a geostrophic correction calculated from the change in the pressure fields. It is shown that updating the velocities is important for the assimilation to be successful. When complete fields of sea surface heights from an identical twin experiment are assimilated the rms error between the model solution and the "true" ocean for the upper-layer pressure field is reduced to less than 5% after six weeks of assimilation. Assimilation of simulated observations along Geosat-ERM and Topex/Poseidon tracks show that both satellites give similar levels of rms error at the end of the assimilation period. The effect of assimilating altimeter data from two satellites is also discussed. The results show there can be a reduction in the rms error of up to 40% with the addition of a second satellite with appropriate orbital characteristics.

1. Introduction

In recent years there has been an increasing interest in data assimilation in ocean models. The goal of assimilation is to improve the numerical solution so that the model produces the "best" realization of the synoptic state of the ocean. The "best" solution usually requires the model solution to be close to the observations in a least-squares sense. Different approaches to the problem of assimilation have been investigated with assimilation algorithms ranging from simple methods such as "nudging" (Malanotte-Rizzoli and Holland 1986, 1988; Holland and Malanotte-Rizzoli 1989; Malanotte-Rizzoli et al. 1989; White et al. 1990a,b,c; Verron 1990; Haines 1991) to more sophisticated algorithms such as Kalman filtering, inverse methods, or variational data assimilation techniques (adjoint techniques) (Bennett and McIntosh 1982; Provost and Salmon 1986; Miller 1986, 1990; Bennett and Budgell 1987, 1989; Thacker and Long 1988; Miller and Cane 1989; Sheinbaum and Anderson 1990a,b; Smedstad and O'Brien 1991; Bennett and Thorburn 1992). Ghil and Malanotte-Rizzoli (1991) give an overview of data assimilation in both meteorology and oceanography.

The similarities and differences between the assimilation techniques can be illustrated by considering the following equation:

$$x_{\text{new}} = x_{\text{model}} + \Delta x, \tag{1.1}$$

where x represents the model variable to be updated. In general, the correction Δx can be represented by three different terms

$$\Delta x = \begin{pmatrix}\text{modulating}\\ \text{matrix}\end{pmatrix}\begin{pmatrix}\text{apportionating}\\ \text{matrix}\end{pmatrix}\begin{pmatrix}\text{data}\\ \text{residuals}\end{pmatrix}. \tag{1.2}$$

The first term in (1.2), the modulating matrix, gives information about the error in the assimilated field. The second term, the apportionating matrix, defines how the information from the observations is spread among the model variables. The third term, the data

* Naval Research Laboratory Contribution Number NRL/JA/7323-92-0001.

Corresponding author address: Dr. Ole Martin Smedstad, Planning Systems Incorporated, 115 Christian Lane, Slidell, LA 70458.

residuals, contains the information from the observations, including noise.

In this context the different assimilation schemes are represented by the following expressions for the modulating and apportionating matrices:

data insertion:

modulating matrix = **I**
apportionating matrix = **I**

nudging/optimal interpolation:

modulating matrix = a priori covariance matrix
apportionating matrix = decorrelation scale

inverse methods/Kalman filter:

modulating matrix = covariance matrix
apportionating matrix = $\mathbf{A}^T$

adjoint methods:

modulating matrix = Hessian matrix
apportionating matrix = $\mathbf{B}^T$

where **I** is the identity matrix and **A** is the matrix of partial derivatives of measurements (model observables) with respect to the model variables; **B** = **A** + adjoint equations, and $(\ )^T$ is the transpose.

The first two assimilation techniques are both simple and relatively economical to use: the matrices needed are either the identity matrix or a priori information about covariance matrices of the model and the observational errors. The disadvantage of using these simple methods is that noise in the observations is treated as a part of the observation, and the assimilation technique does not give a new estimate of the error in the final assimilated field. The next two techniques are more complicated to implement and also much more expensive to use. In the inverse method/Kalman–Bucy filter (Kalman 1960; Kalman and Bucy 1961) the covariance function (the covariance of the model/data difference) is used to compute a correction to the model solution. The covariance function is updated at each time step, and for large numerical models, matrices with more than 10^7 elements need to be inverted. Variational data assimilation techniques are also computationally expensive to use. In this technique the numerical model and its adjoint are integrated together in order to find the optimal solution. Depending on how rapidly the procedure converges, the technique may require several integrations of the model and its adjoint. Thacker (1989) discusses the role of the Hessian matrix and shows that the matrix can be identified as the inverse of the covariance matrix. The advantage of using either the inverse method/Kalman filter or an adjoint method to assimilate observations is that data noise effects are taken into account in the estimation of the model variables, and at the end of the assimilation period the techniques give an estimate of the error in the final model fields. Thacker (1986) discusses relationships between statistical and deterministic methods of data assimilation.

In the literature there have been several papers on assimilation of observations into quasigeostrophic (QG) models. An algorithm that works for a QG model may not give similar results if it is used in a primitive equation (PE) model. In a QG model the streamfunction, which is the only variable, is updated during the assimilation process. In a PE model the variable that is updated is usually the free surface elevation. A change in the free surface elevation according to the data assimilation procedure may result in an imbalance between the model variables, and gravity waves excited by this imbalance may ruin the results of the assimilation. Although a QG model is easier to update, only one variable, the direct observable from altimetry is usually one of the variables of a PE model. Not having to calculate quantities involving derivatives of sparse observations has clear advantages.

There are several approaches that can be followed when observations are assimilated into a numerical model. Data assimilation can be used to determine the initial conditions of a numerical forecast or to continuously update a numerical model during the integration. Another approach is to use data assimilation to estimate parameters in the numerical model. Data assimilation can also be thought of as a way to dynamically interpolate observations onto a regular grid. White et al. (1990c) compared the dynamically interpolated fields from a data assimilation of U.S. Navy Geosat-ERM (Geodetic Satellite-Exact Repeat Mission, Born et al. 1987) sea surface elevation observations into a QG model of the California Current system, with the results from a statistical interpolation method. Their results showed that the dynamical interpolation gave marked improvements in resolution, intensity, and gradient structure of the mesoscale eddy activity. Another advantage of the dynamical interpolation method is that it gives information not only at the sea surface, but is able to estimate the vertical structure of the current system. The determination of the vertical structure depends on the vertical resolution of the numerical model, and the model/assimilation technique's ability to transfer the surface information to the deep ocean.

Numerical ocean models in use today have several layers (or levels) in the vertical. Since an observation from a satellite gives only information about the sea surface, an important question is how to transfer this surface information as fast as possible to the lower layers (levels). The models are able to dynamically transfer the information to the deep ocean (Hurlburt 1986), but the time scale is often too long for the process to be effective if observations are only available over a limited time period. Different approaches have been taken to overcome this problem. Hurlburt et al. (1990) have developed a statistical inference technique where the information from sea surface height observations

is used to infer the lower-layer pressure of a two-layer PE model. Long model simulations were used to derive statistical relationships between the subthermocline pressure at each point in the model and the surface pressure at an array of grid points. This technique has been successfully used to initialize the model with oceanic data and has been shown to significantly improve the forecast skill of the model (Fox et al. 1992a,b). Mellor and Ezer (1991) used a technique, in which model fields were used to calculate correlations between the free surface and subsurface anomalies in temperature and salinity. The calculated correlations and estimated model and data errors were the basis for an optimal interpolation assimilation scheme. In Mellor and Ezer (1991) only data at one point at the sea surface were used in the downward projection, while Hurlburt et al. (1990) used an area in the form of EOFs (empirical orthogonal functions) in the calculations of their coefficients. Haines (1991) also has addressed the problem of transferring surface information to the deep ocean.

In the present assimilation study a realistic two-layer primitive equation model of the Gulf Stream is used (Hurlburt and Thompson 1980; Thompson and Schmitz 1989; Wallcraft 1991). The complexity of the numerical model (nonlinear dynamics and fine grid resolution) makes it necessary to choose a relatively simple and economical assimilation technique. The assimilation algorithm is a variation on the nudging technique, which has been successfully used by several authors (e.g., Holland and Malanotte-Rizzoli 1989; Malanotte-Rizzoli et al. 1989; Verron 1990; White 1990a,b,c). The implementation of the technique in this paper has two modifications compared to the previous studies. One modification consists of the way the nudging term is calculated. The main interest of this paper is short term (a few weeks) mesoscale ocean forecasting and on this time scale the dynamical transfer of surface information to the deep ocean is not very effective. Therefore, the second modification is to use the statistical inference technique of Hurlburt et al. (1990) to update the lower-layer pressure field of the model.

The focus of this paper is on assimilating altimeter data: a complete field of simulated sea surface height is used to explore the effectiveness of the assimilation technique, and simulated altimeter observations along satellite tracks are used to explore the effect of sampling. Several experiments are performed to investigate different aspects of assimilating data into the model. The effect of updating only the upper-layer variables, updating both upper- and lower-layer variables, and the effect of updating the velocities with a geostrophic correction is discussed. Two different satellites are simulated: one with an orbit similar to the Geosat-ERM, and a second satellite with an orbit similar to Topex/Poseidon (Topographic Experiment). The effect of the satellite repeat period on the assimilation is discussed. Experiments quantifying the advantage of having two Geosat-ERM, two Topex/Poseidon, or one Geosat-ERM and one Topex/Poseidon satellite flying at the same time are also discussed. The effects of errors in the observations are addressed in section 3b(3).

A short description of the two-layer hydrodynamic model of the Gulf Stream region is given in section 2. The approach to the problem of assimilating altimeter observations in the numerical model is discussed here, as well as the identical twin observations used in the experiments. The diagnostics used to monitor the convergence of the model solution toward the observations are also described. In section 3 the numerical results using the updating scheme are discussed. The results are summarized in section 4.

2. Specification of the problem

a. The numerical model

The model used here is the Navy Layered Ocean Model. This model is based on the primitive equation model of Hurlburt and Thompson (1980) and has been significantly extended by Wallcraft (1991). A two-layer hydrodynamic version was set up for the Gulf Stream in a manner similar to Thompson and Schmitz (1989). The model domain extends from 78°W to 45°W and from 30°N to 45°N and the gridspacing is $1/8° \times 1/6°$ (latitude, longitude). Figure 1 shows the model domain and the bottom topography. At the solid boundaries a no-slip boundary condition is used. There are four open boundaries in the model. The eastern boundary of the model domain is an open outflow boundary where a variant of the Orlanski (1976) radiation condition is used (Thompson and Schmitz 1989). In addition there is an outflow port in the lower layer at the southern boundary in the western corner of the domain. There are two inflow ports, one in the upper layer in the southwest corner of the model prescribing the transport of the Gulf Stream and one inflow port in the lower layer in the northeastern corner prescribing the transport of the deep western boundary current (DWBC). This current is critical for the separation of the Gulf Stream off Cape Hatteras (Thompson and Schmitz 1989). The DWBC is imposed as a deep inflow via a stream 100 km wide centered near the 3000-m isobath with a parabolic transport distribution. A transport of 20 Sv ($Sv = 10^6\ m^3\ s^{-1}$) is used. This model is used in daily operational forecasts of the Gulf Stream for the Navy (Fox et al. 1992a,b).

The model is a nonlinear primitive equation model with two active layers in the vertical. The model has a free surface and realistic bottom topography in the lower layer. The vertically integrated equations of motion for the two-layer ($n = 2$) finite depth hydrodynamic model are (for $k = 1, 2$)

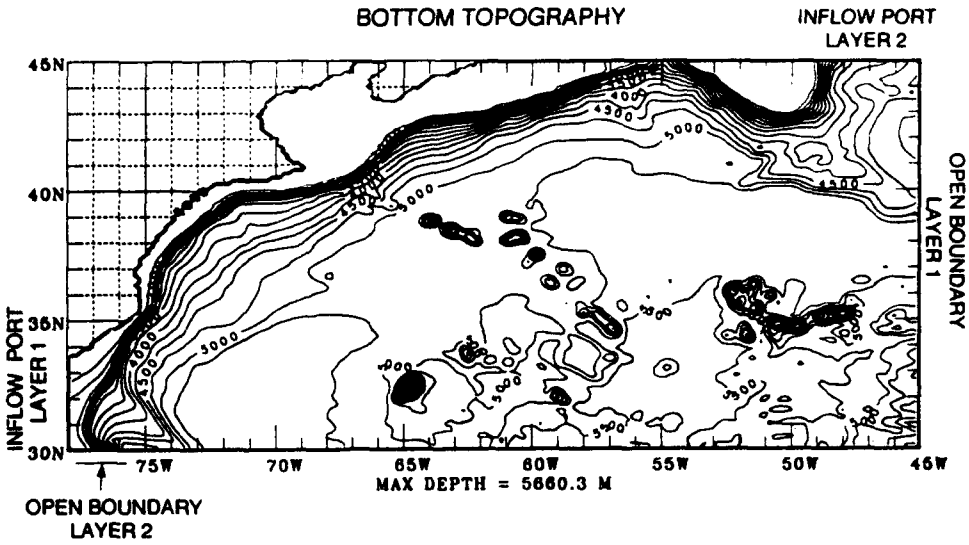

FIG. 1. The geometry and bottom topography of the Gulf Stream model. The grid resolution is 1/8° in latitude and 1/6° in longitude. Contour interval is 250.0 m.

$$\frac{\partial \mathbf{V}_k}{\partial t} + (\nabla \cdot \mathbf{V}_k + \mathbf{V}_k \cdot \nabla)\mathbf{v}_k + \mathbf{k} \times f\mathbf{V}_k = -h_k \sum_{l=1}^{n} G_{kl} \nabla (h_l - H_l) + \frac{(\tau_{k-1} - \tau_k)}{\rho_0} + A_H h_k \nabla^2 \mathbf{v}_k, \quad (2.1)$$

$$\frac{\partial h_k}{\partial t} + \nabla \cdot \mathbf{V}_k = 0, \quad (2.2)$$

where $\mathbf{V}_k = h_k \mathbf{v}_k$ is the transport in the two layers, h_k is the kth layer thickness, H_k is the kth layer thickness at rest, ρ_k is the kth layer density, constant in space and time, f is the Coriolis parameter, and A_H is the coefficient of horizontal eddy viscosity. Also,

$$H_2 = D(x, y) - H_1$$

$$G_{kl} = g, \; l \leq k$$

$$G_{kl} = g - g(\rho_l - \rho_k)/\rho_0, \; l > k$$

$$\tau_0 = \tau_w$$

$$\tau_k = C_k \rho_0 |\mathbf{v}_k - \mathbf{v}_{k+1}|(\mathbf{v}_k - \mathbf{v}_{k+1}), \; k = 1, \cdots, n-1$$

$$\tau_n = C_b \rho_0 |\mathbf{v}_n| \mathbf{v}_n,$$

where $D(x, y)$ is the depth of the bottom topography, τ_w represents the wind stress, C_k is a drag coefficient between the layers, C_b is a drag coefficient at the bottom, $\mathbf{v}_k$ is the velocity in the kth layer, and ρ_0 is a background, average density.

b. *The assimilation technique*

The assimilation algorithm is a nudging technique, Kistler (1974) and Anthes (1974). The nudging scheme can be written

$$\alpha^{\text{new}}(t) = \alpha^{\text{model}}(t) + K(x, y, t)(\alpha^{\text{obs}}(t_0) - \alpha^{\text{model}}(t_0)), \quad (2.3)$$

where α represents the model variable to be updated, t_0 is the time of the observation, and K is a relaxation factor determining the strength of the nudging; K can be a function of both space and time.

In most nudging techniques described in the literature, the last term in (2.3) is calculated at every time step of the assimilation, that is $\alpha^{\text{model}}(t)$ is used. In the case where the observations and the model solution are identical, the last term in (2.3) is exactly zero only at the time of the observation. If K is a function of x, y, and t, spreading the information at the observed point in space and time, the model solution will change even if the observations and the model solution are identical. In the experiments described here, this is avoided by calculating the difference only once, at the time of the observation, t_0. The differences between the two methods are explored in one of the experiments.

Satellite altimetry provides data for the sea surface height, which in the layered model is calculated from the sum of the individual layer thicknesses. It is useful to write the model variables in terms of the pressure in the two layers. The relationship between the pressures, the layer thicknesses, and the sea surface height is given by

$$p_1 = g(h_1 + h_2) = g\eta \quad (2.4)$$

$$p_2 = g(h_1 + h_2) - g'h_1, \quad (2.5)$$

where $g' = g\Delta\rho/\rho$, η is the sea surface height, while h_1 and h_2 are the thicknesses of the upper and lower layer, respectively. The layer thicknesses in terms of the pressures are therefore given by

$$h_1 = \frac{1}{g'}(p_1 - p_2) \tag{2.6}$$

$$h_2 = \left(\frac{1}{g} - \frac{1}{g'}\right)p_1 + \frac{p_2}{g'}. \tag{2.7}$$

The difference between the model and the observed sea surface height is used to update the model. That is, $\Delta\eta = \eta_{obs} - \eta_{model}$ is used to calculate a correction to the upper-layer pressure field (Δp_1) in (2.4). As can be seen from (2.4) and (2.5) an observation of the sea surface height will not by itself determine the pressure in the lower layer. The simplest algorithm, reduced gravity updating, updates only the pressure in the upper layer, and the correction to the pressure in the lower layer is set equal to zero ($\Delta p_2 = 0$). From (2.6)–(2.7) the expressions for the corrections, Δh_1 and Δh_2, to h_1 and h_2 are in the case of reduced gravity updating

$$\Delta h_1 = \frac{\Delta p_1}{g'} = \frac{\rho}{\Delta\rho}\Delta\eta \tag{2.8}$$

$$\Delta h_2 = \left(\frac{1}{g} - \frac{1}{g'}\right)\Delta p_1 = \left(1 - \frac{\rho}{\Delta\rho}\right)\Delta\eta. \tag{2.9}$$

Earlier studies have shown that it is important to transfer information about changes in the upper-layer pressure field to the lower layer (Hurlburt 1986; Hurlburt et al. 1990; Haines 1991). Hurlburt et al. (1990) investigated the use of a statistical technique to infer the subthermocline pressure anomalies from upper-layer anomalies (sea surface height data). Although there is only a weak correlation between the upper- and lower-layer pressure fields at each point of the model, the lower-layer pressure could be accurately inferred by relating it to empirical orthogonal functions derived from a grid of points in the upper layer. Fox et al. (1992a,b) have shown that using the statistical inference technique significantly improves the forecast skill of the Gulf Stream model when real oceanic data are used. The statistical inference technique of Hurlburt et al. (1990) is used in the assimilation experiments described in the next section. The correction to the pressure in the upper layer is used to infer the correction to the pressure in the lower layer of the model, and the expressions in (2.6) and (2.7) are used to calculate the corrections to the layer thicknesses.

Updating only the layer thicknesses results in dynamically unbalanced model fields. This problem is reduced by updating the velocities, u and v, with a geostrophic correction according to

$$\Delta u_{gk} = -\frac{1}{f}\frac{\partial\Delta p_k}{\partial y} \tag{2.10}$$

$$\Delta v_{gk} = \frac{1}{f}\frac{\partial\Delta p_k}{\partial x}, \tag{2.11}$$

where $k = 1, 2$. The correction is applied only to the upper layer if $\Delta p_2 = 0$, or to both layers if the statistical inference technique is used to update the lower-layer pressure field.

The performance of the assimilation algorithm is monitored by calculating the rms error for the various fields. The rms error is given by

$$\text{rms} = \left(\frac{\sum_{i=1}^{N_x}\sum_{j=1}^{N_y}(\phi_{i,j}^{model} - \phi_{i,j}^{obs})^2}{N_x N_y}\right)^{1/2}. \tag{2.12}$$

The error is evaluated over the entire domain of ocean points. Here, $\phi_{i,j}^{model}$ and $\phi_{i,j}^{obs}$ are the fields in the assimilation run and control run, respectively. In addition the error in the position of the axis of the Gulf Stream is calculated. The error is the mean error in the position of the stream between 73°W and 50°W.

c. *The observations*

In the experiments, identical twin data are used as "observations," which means the quantities to be assimilated are solutions of the model. In some cases noise is added. The use of identical twin data makes it possible to evaluate the effectiveness of the assimilation in constraining the evolution of the numerical model. Since the "observations" are extracted from the same model as the one used in the assimilation experiments, the dataset and the model solution are dynamically consistent. In the first experiments, perfect observations are assimilated, that is, the observations are extracted directly from the control run. In reality perfect observations do not exist, but it is important to test the model and the assimilation scheme's performance with perfect observations both in the sense of no errors and dynamical consistency. This is the best scenario one can expect and the errors represent lower limits for the assimilation of real sea surface height observations.

The question on how errors in the observed field will influence the assimilation is also discussed. Even with noise-free simulated altimetry, the sampling characteristics of the satellite will induce errors due to aliasing of features smaller than the track spacing. In addition to this "error," correlated and uncorrelated noise is added to the simulated altimetry in some experiments.

For the assimilation results not to depend on one particular model realization, seven independent experiments are performed. The model is integrated from different spunup states to create what is called the "true" ocean. A complete sea surface height field is saved at 6-day intervals. Experiments with intervals between 2 and 8 days showed that the results were not very sensitive to this choice. The rms error reached the same level at the end of the assimilation. In addition, observations of the sea surface height along the tracks of two simulated satellite orbits are extracted from the "true" ocean. The first satellite simulates the Geosat-ERM mission with a repeat period of approximately 17 days, while the second satellite has a repeat period of approximately 10 days similar to the Topex/Posei-

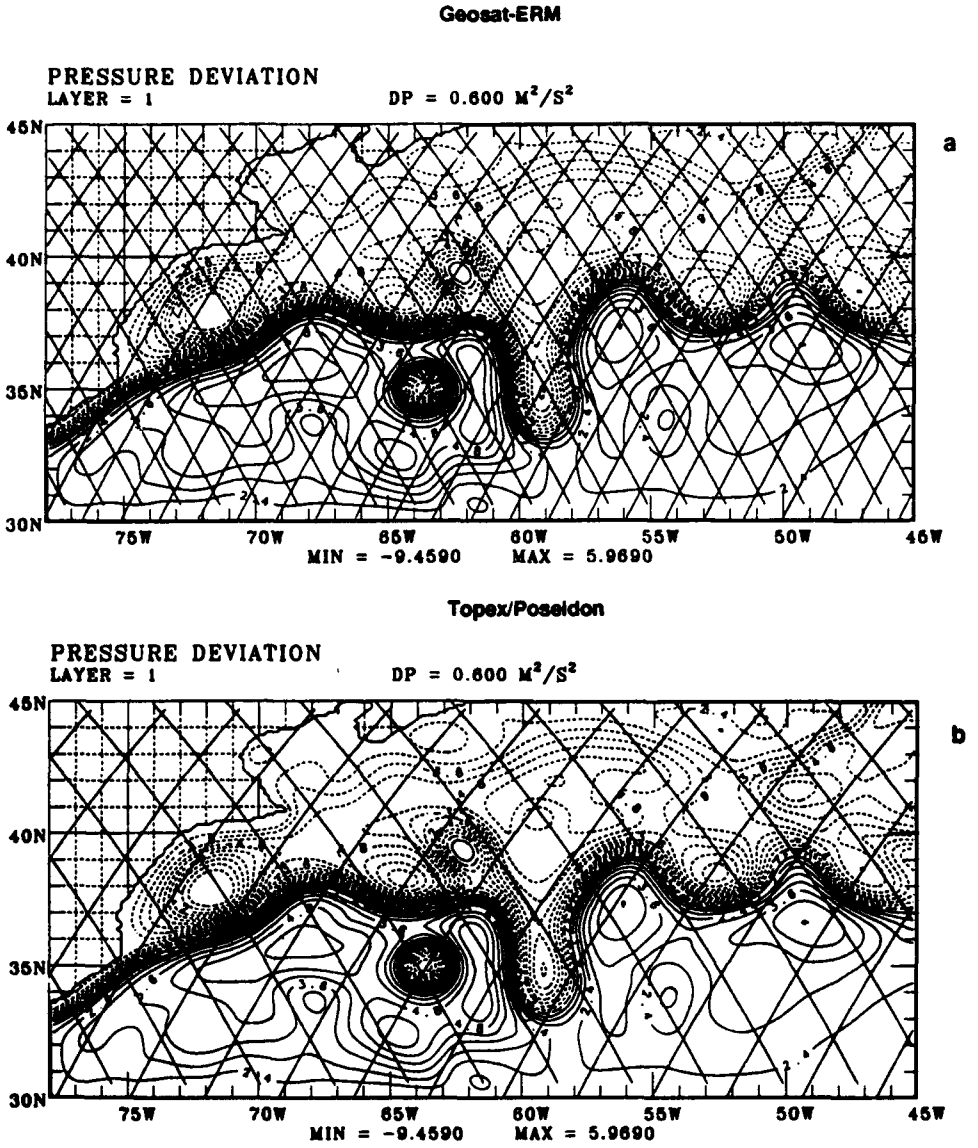

FIG. 2. The satellite tracks for a complete repeat cycle for the two different orbits used in the assimilation. (a) The 17-day repeat cycle Geosat-ERM tracks, (b) the 10-day Topex/Poseidon tracks. The background upper-layer pressure field is one of the initial model fields used to create the true ocean.

don mission. Holland and Malanotte-Rizzoli (1989) and Verron (1990) used similar satellites in their assimilation studies using a QG model. Even with noise-free simulated altimetry, the sampling characteristics of the satellite will induce errors due to aliasing of features smaller than the track spacing. In addition to this "error," correlated and uncorrelated noise is added to the simulated altimetry in some experiments.

Observations of the sea surface height at the track positions intersecting the model domain are collected once a day. There is little variability on a 1-day time scale and this is used as justification for collecting data only once a day. The model domain is typically intersected by three tracks each day. The track sequence is realistic. Figures 2a,b show the Geosat-ERM and Topex/Poseidon satellite tracks covering the model domain, respectively. The background upper-layer pressure field is the initial day from one of the integrations performed to create the "true" ocean. The figures show the tracks for a complete repeat cycle, 17 days for Geosat-ERM and 10 days for Topex/Poseidon. The track separation of approximately 1.5° for Geosat-ERM at 30°N and 3.0° for Topex/Poseidon is observed. It is also worth noting that for the Topex/Poseidon repeat period, it is possible for the satellite to completely miss rings separated from the Gulf Stream (e.g., near the center of Fig. 2b). Rings and other features do not appear and disappear independently, however. A ring

will tend to persist for weeks or months, will gradually move, and will have come into existence only after a period of increasing meandering of the stream itself. By integrating the observations with an assimilation scheme and a realistic circulation model, features which initially would seem to be aliased or missed completely may be accurately represented.

The question of how additional information from two Geosat-ERM, two Topex/Poseidon, or a combination of the two satellites influences the assimilation is also addressed. Observations are extracted along the tracks of the two satellites flying in exactly the same orbit, but offset in time so that they are approximately 8.5 days out of phase for the Geosat-ERM and 5 days for the Topex/Poseidon. This corresponds to one-half repeat orbital period for the two satellites. These experiments increase the temporal sampling of the data. Two additional experiments are performed. The satellites either fly side by side in orbits offset in space by half the distance between the tracks (increasing the spatial sampling) or the satellite in one of the orbits is offset in time like in the first experiment (increasing both temporal and spatial sampling).

The seven assimilation experiments are run for a period of 6 weeks. One of the seven experiments was run for a whole year to check the level of convergence reached at the end of the 6-week assimilation. The results (not shown) show that the 6-week period is long enough for the results to be nearly asymptotic. The level of convergence for the 6-week experiments will be compared to the 1-year results. The initial day for each of the assimilation experiments is chosen so that deviations from the model mean for the initial and "true" ocean fields are uncorrelated.

3. Numerical results

Table 1 lists the different experiments performed. Before the assimilation experiments are described, the results from the integrations with no assimilation (case 0) are discussed. Figures 3a,b show the difference in the upper- and lower-layer pressure field between the "true" ocean and the model solution from one of the experiments. The last day of the 6-week integration is shown. There are significant differences between the "true" ocean and the model solution. Most of the differences are located along the Gulf Stream front, especially in the upper layer. The differences in the pressure fields in each layer are of the same order of magnitude as the total pressure in that layer. In Figs. 4a,b the global rms error [Eq. (2.3)] is shown for the pressures and the U (zonal) transports, respectively (case 0). If not otherwise stated the rms error shown in the next sections is the average error for the seven independent experiments. The rms errors are scaled by the variance of the "true" ocean field. Only the rms error for the U transports is shown since both the U and the V (meridional) transports have a similar behavior. During the 6-week period the rms error is nearly constant and the deviations from the temporal mean field of the model solution and the "true" ocean are uncorrelated. The average positional error of the axis of the Gulf Stream for case 0 is given in Table 2. The error is close to 80 km during the entire 6-week integration.

a. Complete field of sea surface height observations

The first set of experiments is designed to isolate the effects of choosing a particular assimilation approach. While holding the spatial/temporal distribution of input data constant (i.e., observations on a uniform grid every 6 days), the following effects are examined.

case 1: updating only the upper-layer pressure and velocity field
case 2: statistical transfer of p_1 into p_2 and updating the velocity fields
case 3: update p_1 and p_2 but no geostrophic update of the velocities
case 4: same as case 2 but calculating nudging term at every time step.

In the experiments where a complete field of observations are used, the relaxation factor K in Eq. (2.3) is a function of time only. One question that arises is how fast should the information in the observations be "nudged" into the model. In practice, it is not possible to update the model only when a new observation becomes available ($K = 1$ at the point in time and space of the observation and $K = 0$ everywhere else). A numerical model and especially a primitive equation model is sensitive to sudden changes in the model fields, and a direct insertion of an observation creates a shock to the model. In severe cases when the difference between the model and the observation is large, the result can be an unstable solution. Therefore, it is necessary to spread the information over several time steps. The goal is to nudge the information into the model as rapidly as possible without destroying the numerical solution. The data must be sufficiently spread over time (and space if data is not on a uniform grid) so that geostrophic adjustment can occur without generation of significant gravity waves and viscosity will not quickly damp out the information because it is on a small scale. Several experiments not described here were performed to test the sensitivity of the assimilation to the choice of interval over which the model fields are updated. The results showed that the model is not very sensitive to this interval. Periods between 1 and 6 days were tested, and only small differences in the final solution were found. In the results described here the complete fields of observations are inserted into the model over a period of 2 days. This interval gave a smooth model evolution with only a minimal number of gravity waves excited. Holland and Malanotte-Rizzoli (1989) and Verron (1992) also found that a period

TABLE 1. The assimilation experiments.

Case	Observations	Nudging term	Update				Number of experiments
			$p1$	$p2$	U1V1	U2V2	
0	No observations	—	no	no	no	no	7
1	Complete field of SSH No errors	Calculated once	yes	no	yes	no	7
2	Complete field of SSH No errors	Calculated once	yes	yes	yes	yes	7
3	Complete field of SSH No errors	Calculated once	yes	yes	no	no	7
4	Complete field of SSH No errors	Calculated every time step	yes	yes	yes	yes	7
5	One simulated Geosat-ERM No errors	Calculated once	yes	yes	yes	yes	7
6	One simulated Topex/Poseidon No errors	Calculated once	yes	yes	yes	yes	7
7	Two simulated Geosat-ERM Offset in time No errors	Calculated once	yes	yes	yes	yes	7
8	Two simulated Topex/Poseidon Offset in time No errors	Calculated once	yes	yes	yes	yes	7
9	Two simulated Geosat-ERM Offset in space No errors	Calculated once	yes	yes	yes	yes	7
10	Two simulated Topex/Poseidon Offset in space No errors	Calculated once	yes	yes	yes	yes	7
11	Two simulated Geosat-ERM Offset in space and time No errors	Calculated once	yes	yes	yes	yes	7
12	Two simulated Topex/Poseidon Offset in space and time No errors	Calculated once	yes	yes	yes	yes	7
13	One simulated Geosat-ERM One simulated Topex/Poseidon No errors	Calculated once	yes	yes	yes	yes	7
14	One simulated Geosat-ERM Rms error of 5 cm Decorrelation scale $\approx$ 200 km	Calculated once	yes	yes	yes	yes	7
15	One simulated Topex/Poseidon Rms error of 5 cm Decorrelation scale $\approx$ 200 km	Calculated once	yes	yes	yes	yes	7

of 2 days gave good results in their QG model assimilations. The data are inserted into the model at a constant rate over the 2-day period (K = const for 2 days). Experiments using different functional forms were performed, but the results were not significantly different.

1) CASE 1: UPDATE PRESSURE AND VELOCITIES IN UPPER LAYER ONLY

The simplest assimilation that can be performed is to update only the upper-layer variables of the model. In the first experiment, the p_1 field is updated and a geostrophic correction to the velocities in the upper layer is calculated. No updating is performed to the lower-layer pressure and velocity field. Figures 4a,b show the global rms error for the pressures and U transports, respectively (case 1). The rms error for the upper-layer pressure is reduced to about 15% at the end of the assimilation period with most of the reduction occurring during the first week of assimilation. During the succeeding 5 weeks only a small decrease is observed. The results for the lower-layer pressure show little improvement in terms of the rms error. The U transports behave similarly although the reduction in the rms error is less than for the pressure field. This can be explained by the fact that the velocity (transport) in the model is not an observable, whereas p_1 is directly proportional to the sea surface height. The reduction in rms error for a variable that is not an observable is not expected to be as large as for a direct observable. The difference between the "true" ocean and the model solution for the p_1 and p_2 fields for one of the seven independent experiments is shown in Figs. 5a,b. The figures show the difference at the last day of the assimilation. Figures 3a,b show the corresponding difference

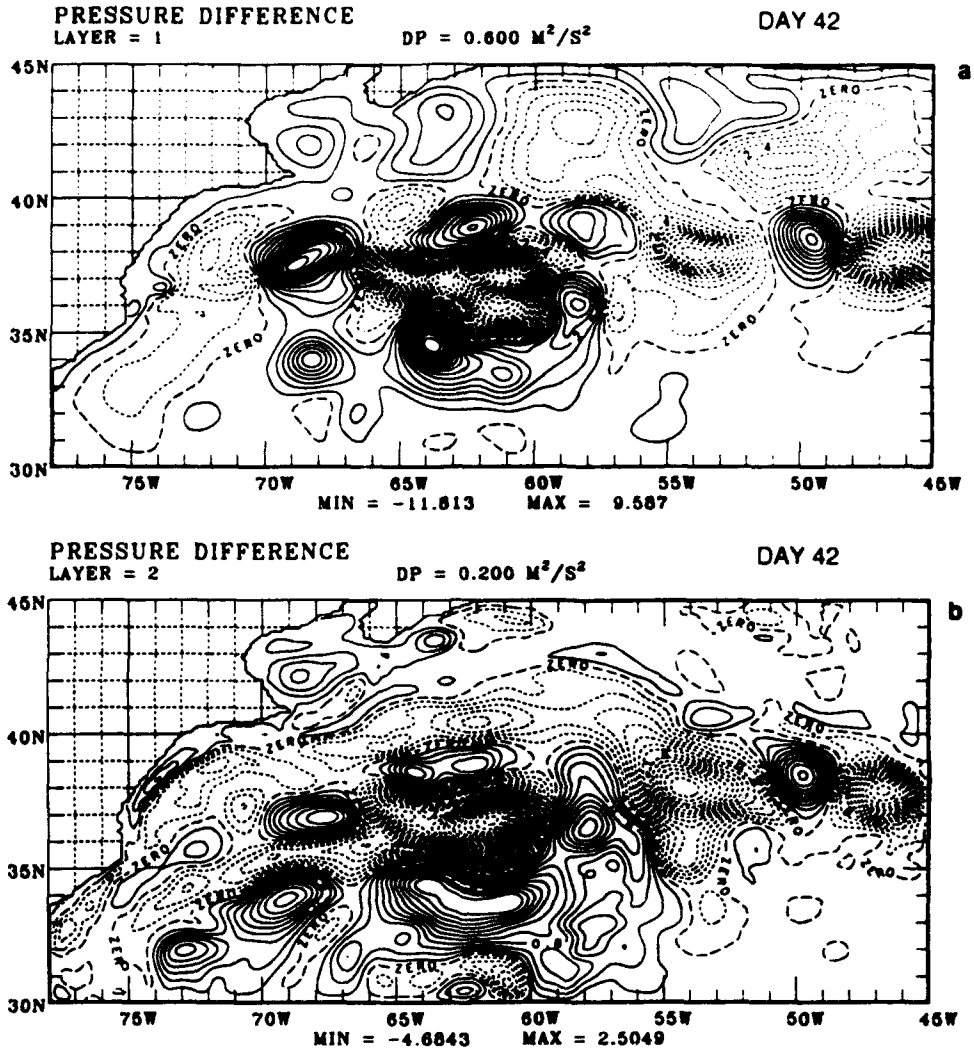

FIG. 3. The difference between the true ocean and the model solution of the p_1 and p_2 fields is shown for one of the experiments where no assimilation is performed (case 0): (a) p_1 at day 42 and (b) p_2 at day 42.

in the case 0 experiment. The error in the p_1 field has decreased during the assimilation period, but there are still differences along the axis of the Gulf Stream. The results for the lower layer show only a small improvement. Table 2 gives the error in the axis of the Gulf Stream (case 1). The error decreases to approximately 12 km at the end of the assimilation.

On a time scale of a few weeks the dynamical transfer of surface information to the deep layer is not efficient enough to have an impact on the evolution of the lower-layer fields. In fact, it may not converge at all [see Hurlburt et al. (1990) for a discussion of the conditions for convergence in the dynamical scheme]. Comparing these results to the 1-year experiment, shows that the rms error in the upper-layer pressure does not decrease below the level reached at the end of the 6-week period. The rms error of the lower-layer pressure does vary during the yearlong integration, but the level of rms error does not decrease significantly below the 6-week level. The transports have also reached their level of convergence at the end of the 6 weeks.

2) CASE 2: UPDATE PRESSURES AND VELOCITIES IN BOTH LAYERS

In the next experiment, the statistical inference technique is used to infer the correction to the lower-layer pressure field. This correction is used to calculate a geostrophic correction for the velocity in the lower layer. Figures 4c,d show the global rms error for the pressures and the U transports, respectively (case 2). In this case the rms error for the upper-layer pressure decreases to about 3% at the end of the 6-week assimilation period. Again, most of the reduction occurs during the first week of the assimilation. The additional information given to the lower layer through the in-

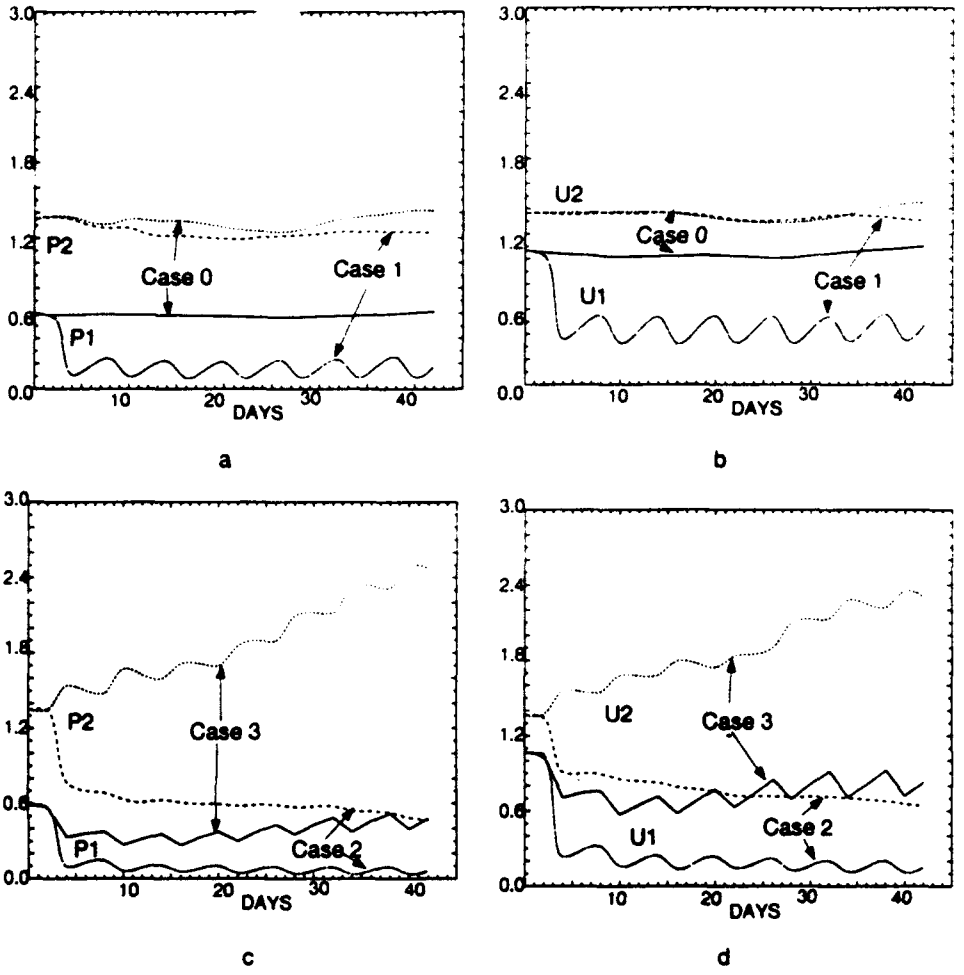

FIG. 4. The time evolution of the global rms error for the pressure and U transport in the two layers for four different cases: case 0, no assimilation; case 1, only the upper-layer pressure and velocity field is updated; case 2, the statistical inference technique is used to update the lower-layer pressure; case 3, the pressure in both layers is updated but the velocities are not. The error is scaled by the variance of the true ocean field. The rms error is the average over seven independent experiments. (a) The pressure for cases 0 and 1, (b) the U transport for cases 0 and 1, (c) the pressure for cases 2 and 3, and (d) the U transport for cases 2 and 3.

ference technique forces the rms error in the upper layer to drop to a lower level than in the previous experiment. The most important feature is that now the lower-layer pressure shows a large decrease in the rms error. The decrease is not as pronounced as for the upper-layer pressure, but after 6 weeks the rms error has dropped to about 50%. The reduction in the rms error for the U transport (Fig. 4d) has qualitatively a similar behavior as the pressure field. As explained in the previous experiment, the decrease is not as large

TABLE 2. The error in the position of the axis of the Gulf Stream for the different cases. The error is given in kilometers and is the average for the seven independent experiments.

	Case															
Day	0	1	2	3	4	5	6	7	8	9	10	11	12	13	14	15
0	77	77	77	77	77	77	77	77	77	77	77	77	77	77	77	77
20	80	25	10	55	20	25	30	15	32	27	25	19	25	20	30	30
42	80	12	5	70	10	27	27	15	25	22	17	19	20	24	30	30

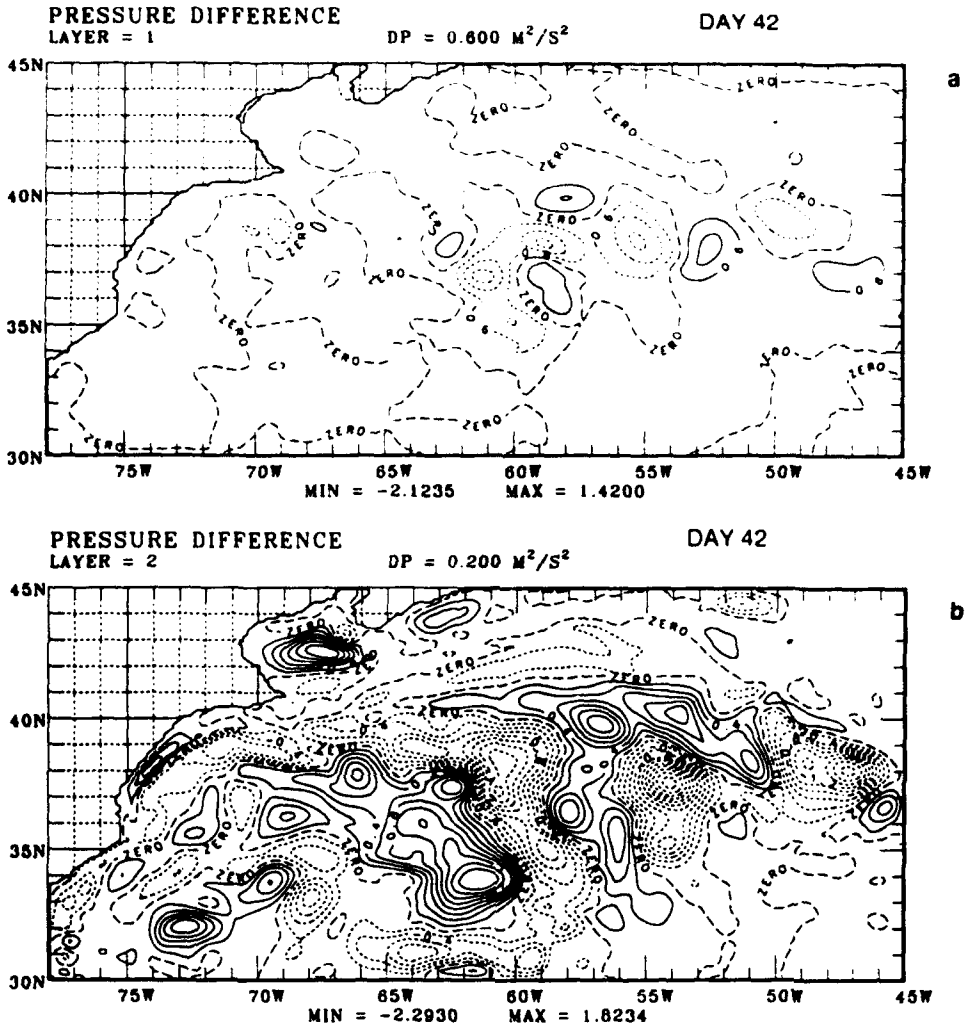

FIG. 5. The difference between the true ocean and the model solution of the p_1 and p_2 fields is shown for one of the case 1 experiments where pressures and velocities in the upper layer only are updated: (a) p_1 after 42 days of assimilation and (b) p_2 after 42 days of assimilation.

as for the pressure. There is, however, a larger decrease than in the first assimilation experiment in which only dynamical transfer of information to the lower layer occurred. The use of the statistical inference technique does not only improve the pressure field in the lower layer, but also the pressure field in the upper layer and the transports in both layers. The statistical inference technique and the dynamics of the model play an important role together. The inference technique makes the model p_2 field close to the "real" p_2 field and then the dynamics of the model can more effectively force the model toward convergence.

The difference between the "true" ocean and the model solution for the p_1 and p_2 fields for one of the independent experiments is shown in Figs. 6a,b. The figures show the difference fields on the last day of the assimilation. The error in the p_1 field shows a larger decrease than in the case 1 experiment (see Fig. 5a). The differences located around the axis of the Gulf Stream have disappeared. The lower-layer pressure field in Fig. 6b shows a much larger decrease in the error than in the case 1 experiment (Fig. 5b). Table 2 gives the axis error for the Gulf Stream (case 2). The error decreases to approximately 5 km. The gridspacing of the model corresponds to 12–15 km, so an error of 5 km is well below the resolution of the model.

Compared to the 1-yr assimilation integration, the rms error of the upper-layer pressure has reached the asymptotic value at the end of the 6-week period. The rms error of the lower-layer pressure slowly decreases another 10% by the end of the year. The transports show a similar behavior. The upper-layer transport has reached the asymptotic value at the end of 6 weeks, while the lower layer slowly decreases another 15%.

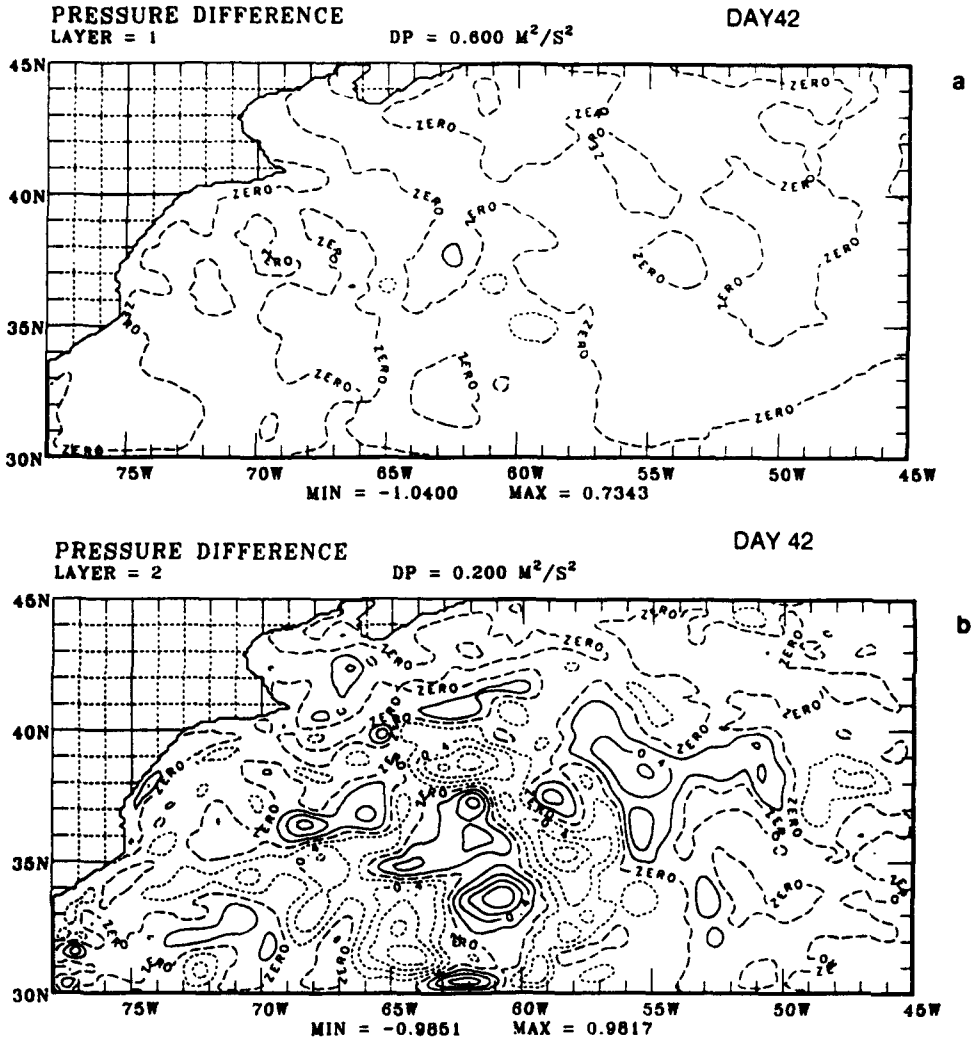

FIG. 6. The difference between the true ocean and the model solution of the p_1 and p_2 fields is shown for one of the case 2 experiments where pressures and velocities in both layers are updated: (a) p_1 after 42 days of assimilation and (b) p_2 after 42 days of assimilation.

3) CASE 3: UPDATE ONLY PRESSURES IN BOTH LAYERS

The effects of updating not only the pressures, but also using a geostrophic correction to update the velocities are investigated in the next experiment. The experiment is similar to case 2, but in this case the velocities are not updated. The rms errors for the pressures and the U transports are shown in Figs. 4c,d, respectively (case 3). Note the change in scale of the vertical axis. Comparing these results with case 2 show that the geostrophic correction has an important effect on the assimilation. After an initial decrease in the rms error in the upper layer during the first 12–14 days of the assimilation, the error starts to increase. In the lower layer there is an increase during the entire period. Investigation of the reason behind this behavior revealed that for the lower-layer pressure field to evolve according to the observations, the geostrophic velocity correction plays an important role. If only the pressure in the lower layer is updated, the velocity field dominates the solution and the mass field adjusts according to the velocity field. An example of this is shown in Figs. 7a–d. The pressure in the lower layer is shown for four different cases. Figure 7a is the pressure field for the "true" ocean, Fig. 7b is the result from the case 0 experiment, Fig. 7c is the result from the case 2 experiment, while Fig. 7d shows the pressure field from the case 3 experiment. The pressure fields are shown at day 4 of the assimilation. The eddy field in case 2 and the "true" ocean are similar. The field in case 3, however, does not resemble the true ocean. In fact it is more like case 0. On the length scales of the eddies in the lower layer, the mass field adjusts to the velocity field. The length scale is much less than the barotropic Rossby radius of deformation, which is the important

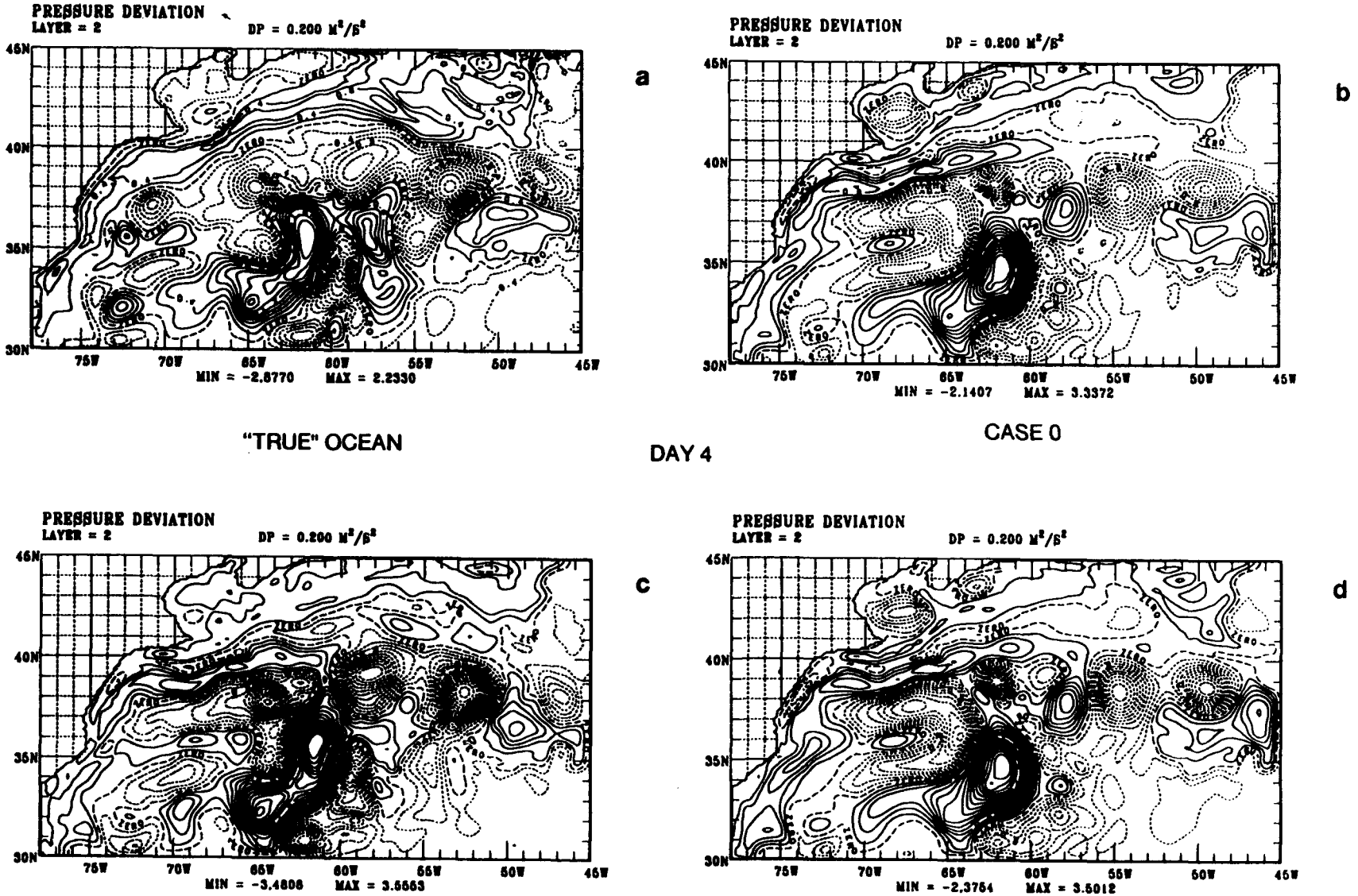

FIG. 7. The lower-layer pressure field from one of the seven experiments. (a) The pressure field for the true ocean; (b) the pressure field for case 0, no updating; (c) the pressure field for case 2, pressures and velocities are updated in both layers; and (d) the pressure field for case 3, only pressures are updated in both layers. The fields are shown at day 4 of the assimilation.

length scale for the lower layer. For the statistical inference to have an impact on the evolution, the velocities in the lower layer must be updated as well.

The axis error is given in Table 2 (case 3). A decrease in the error is observed in the first half of the assimilation, but toward the end the error has increased to 70 km.

The 1-year experiment confirms these results. The model continues to diverge during the whole year.

4) Case 4: Calculate nudging term at every time step

The effect of calculating the nudging term in (2.3) only once, at the time of the observation, is shown in the next experiment. The same seven experiments described in section 3a(1)–(3) are performed with the nudging term recalculated at every time step of the assimilation. The nudging parameters in the previous experiments are used; that is, the data are inserted into the model over a period of 2 days. Figures 8a,b show the rms error for the pressures and U transports for case 4, while Table 2 gives the error in the position of the Gulf Stream. The two methods give similar results but with the method used here giving slightly better values, especially for the transports. The main advantage of calculating the term only once is that the model solution is not changed if the observations are identical to the numerical model solution.

The 1-year assimilation showed a similar behavior as in case 2, where the upper-layer rms errors reached the asymptotic values after 6 weeks, while there is a slow increase in the lower-layer rms error toward the end of the year.

Calculations of standard errors for the different curves in Figs. 4 and 8 show that these errors are small, typically less than 10%. Statistical calculations show that the difference between the results in cases 1–4 are significant with the probability that the results are different being higher than 99.9%.

b. *Observations along satellite tracks*

In light of the results in the previous section, the experiments in this section update the upper- and lower-layer pressure field and the velocities in both layers. In the experiments where the observations are available only along satellite tracks, the information is spread around the tracks. The factor K is in this case an exponential decay function with a spatial decorrelation scale of 150 km and a time decorrelation scale of 5 days. In earlier work White et al. (1990a,b,c) used a time decorrelation scale of 17 days in the California Current region, the repeat cycle of the Geosat-ERM. In the active region of the Gulf Stream this time scale is too long. A typical decorrelation scale for this region is about 10 days (Watts 1983). Different decorrelation scales were tested, but 150 km and 5 days gave the best results.

1) Case 5 and 6: Observations along Geosat-ERM and Topex/Poseidon tracks

The assimilation experiments are carried out in parallel for the two satellites described in section 2c. In the first experiment, perfect "observations" are used. Figures 9a,b show the global rms error for the pressures and U transports for Geosat-ERM (case 5) and Topex/Poseidon (case 6). The rms error after 6 weeks of assimilation has reached a slightly lower level for the Geosat-ERM compared to the Topex/Poseidon. In either case the largest decrease in the rms error occurs during the first 20 days of the assimilation. After the

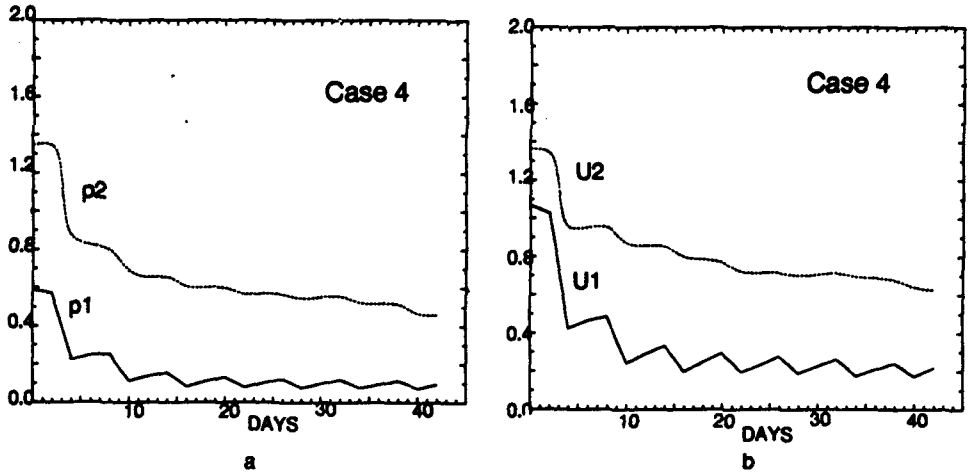

FIG. 8. The time evolution of the global rms error for the pressure and U transport for case 4 where the nudging term is calculated at every time step. The error is scaled by the variance of the true ocean field. (a) The pressure and (b) the U transport.

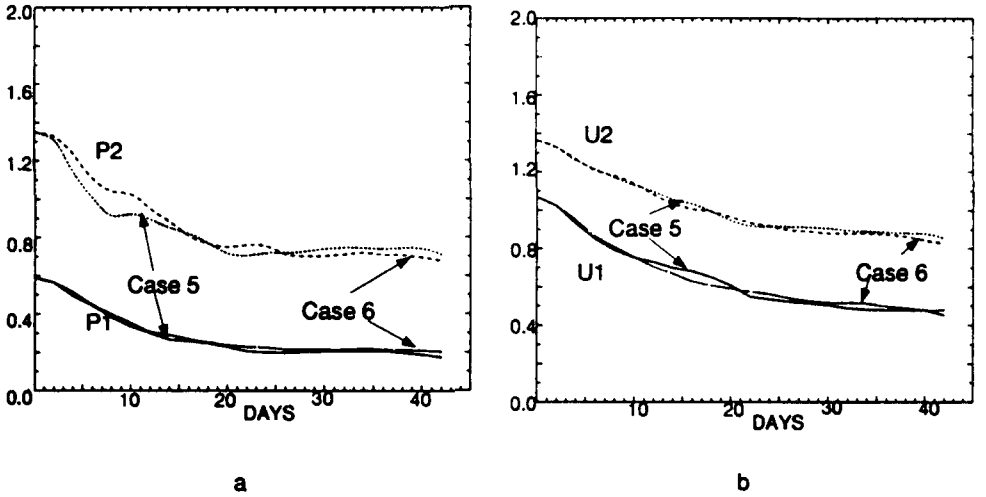

FIG. 9. The time evolution of the global rms error for the pressure and U transport updating the model along Geosat-ERM (case 5) and Topex/Poseidon (case 6) tracks. The error is scaled by the variance of the true ocean field. (a) The pressure for cases 5 and 6 and (b) the U transport for cases 5 and 6.

initial decrease there is a slow convergence toward an equilibrium.

The difference between the true ocean and the model solution of the p_1 field for one of the independent experiments is shown in Figs. 10a,b. Figure 10a shows the results from the Geosat-ERM assimilation, while Fig. 10b shows the results from the Topex/Poseidon experiment. The p_1 difference field for the two satellites has similarities. As expected, the largest differences are located in the vicinity of the most active region of the Gulf Stream. The amplitude of the difference fields for the two cases is about the same. The space scale of the difference field is larger for the Topex/Poseidon satellite. This is due to the coarser space resolution with the 10-day repeat period. In the Topex/Poseidon case there are parts of the domain outside the active region that show larger differences than in the Geosat-ERM case. These results are typical for all the experiments performed.

Table 2 gives the average axis error the Geosat-ERM (case 5) and Topex/Poseidon (case 6) experiments. The error decreases to 27 km for both satellites at the end of the 6-week assimilation period.

Comparing these results to the 1-year integration, both the upper- and lower-layer fields have reached their asymptotic values at the end of the 6-week assimilation period.

The standard errors and the statistical calculations for the results in this section show that it is difficult to distinguish the results from the two satellites. The errors are typically less than 10% for the pressure fields and less than 5% for the transports. The standard error for the position of the Gulf Stream is approximately 4 km for the Geosat-ERM satellite and 2 km for the Topex/Poseidon.

2) CASE 7–13: EFFECTS OF TWO SATELLITES

The question of how an increased sampling in time and space of the sea surface height influences the assimilation is addressed in this section. In these experiments two Geosat-ERM or two Topex/Poseidon satellites are flown over the model domain. Different scenarios are tested to examine the relative importance of spatial and temporal sampling. The first experiment has the two satellites flying in exactly the same orbit, but offset in time so that they are approximately 8.5 days out of phase for the Geosat-ERM and 5 days for the Topex/Poseidon (case 7 and 8) corresponding to one-half the repeat orbital period for the satellites. These experiments increase the temporal sampling of the data. In the second set of experiments, the orbits of the satellites are offset in space so that the second satellite flies in between the tracks of the first satellite. In the experiments the satellites are either flown side by side in the offset tracks (increasing the spatial sampling) (case 9 and 10) or the satellite in one of the orbits are offset in time like in the first experiment (increasing both temporal and spatial sampling) (case 11 and 12). In an additional experiment, a combination of the two satellites is used (case 13). Figures 11a,b show the global rms error for the upper-layer pressure field for four cases, only one satellite (case 5 and 6) and the four experiments described above. Only the upper-layer pressure field is shown to clearly demonstrate the difference between the cases. The error is the average error for the seven experiments. The results show that in the Geosat-ERM case the error minimizes by having the two satellites offset in time. For the Topex/Poseidon satellite on the other hand, most is gained if the two satellites are offset in both time and space. The reason for this difference is the coarser spa-

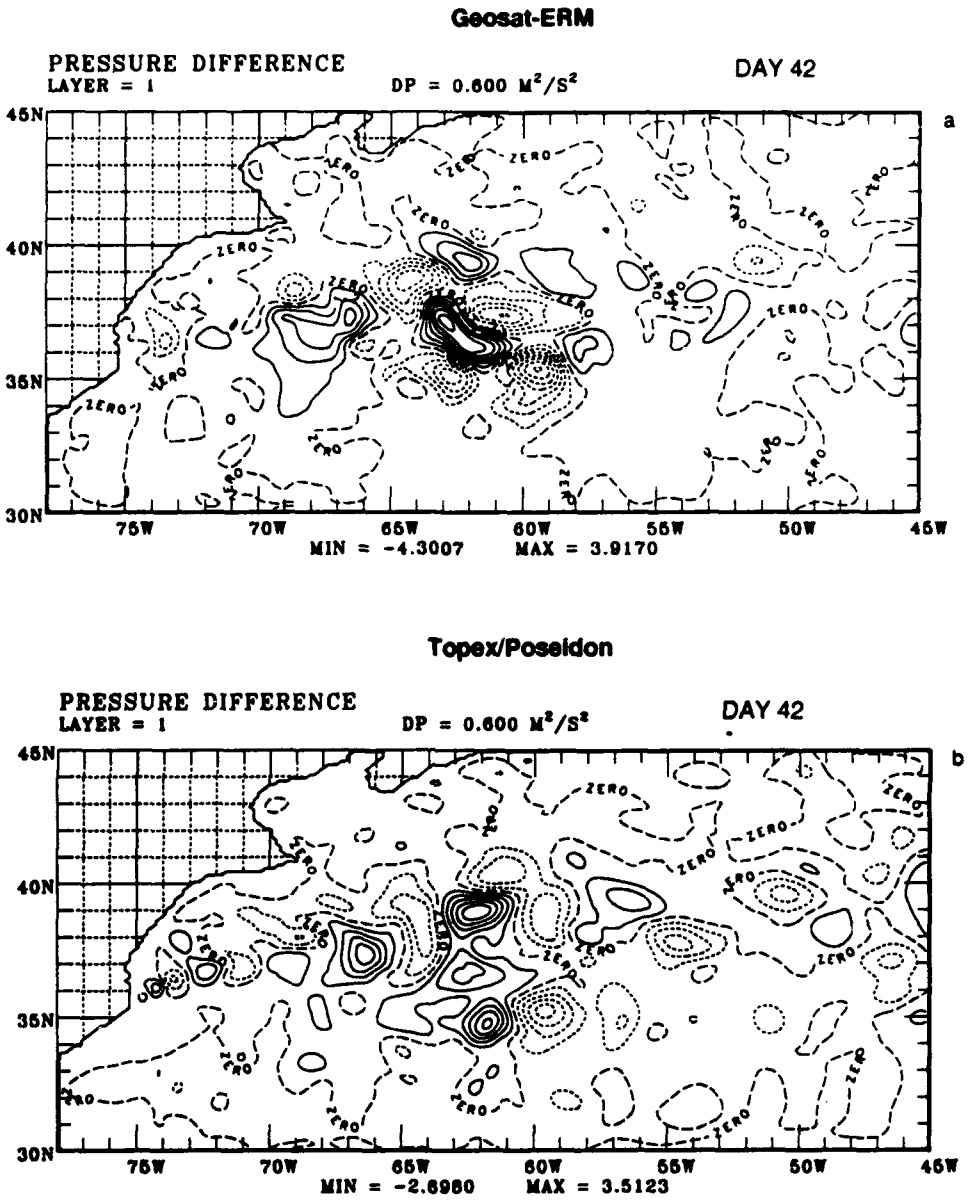

FIG. 10. The difference between the true ocean and the model solution of the p_1 field for one of the experiments where Geosat-ERM and Topex/Poseidon tracks are used in the assimilation: (a) p_1 after 42 days of assimilation along Geosat-ERM tracks and (b) p_1 after 42 days of assimilation along Topex/Poseidon tracks.

tial resolution and higher temporal resolution of the Topex/Poseidon satellite. A combination of the two satellites gives results that are better than just one satellite but not as good as the best results using two satellites of the same type. The results are confirmed by the error in the position of the axis of the Gulf Stream shown in Table 2. Increasing the temporal sampling for the Geosat-ERM (case 7) decreases the axis error to about 15 km compared to 27 km if only one satellite is used. The results for Topex/Poseidon similarly show that increasing both the temporal and spatial sampling (case 12) decreases the axis error to 20 km compared to 27 km with only one satellite. In the case of one Geosat-ERM and one Topex/Poseidon satellite (case 13) the error decreases to 24 km.

The results from the 1-yr assimilation show that the upper-layer variables have reached their asymptotic values after 6 weeks. The lower-layer variables show an additional decrease of 15% by the end of the year.

The standard error for the upper-layer pressure field is less than 10% and less than 2 km for the axis error. Statistical calculations show that the differences be-

tween cases 5 and 13 are significant. The probability that the results are different is higher than 90% for most combinations of two satellites.

3) CASE 14–15: EFFECT OF NOISE IN THE OBSERVATIONS

The previous experiments used perfect "observations," the observations were extracted directly from the model solution. Real data are not noise free, and it is important to know the effect of noise on the assimilation. In the next experiments the effect of noise in the "observations" along satellite tracks is investigated. Two experiments, (results not shown) were performed adding a field of white noise with two different levels of rms error to the "observations" from the Geosat-ERM and the Topex/Poseidon satellites used in cases 5 and 6. An rms error of 5 and 10 cm was used. Adding the white noise error fields to the observations had little effect on the pressure fields for either satellite sampling pattern. These results are consistent with Thompson (1986). His experiments showed the model viscosity quickly damps uncorrelated noise.

The error model of Hurlburt et al. (1990) is used in the next set of experiments. A correlated error field with a decorrelation scale of approximately 200 km and an rms error of 5 cm is added to the "observations." The global rms error as a function of time for the experiments with error added to the "observations" is shown in Figs. 12a–d for the pressures and the transports, case 14 for the Geosat-ERM, and case 15 for the Topex/Poseidon satellite. The results from the experiments with error-free observations are also shown, cases 5 and 6, respectively. In the Geosat-ERM case, the inclusion of the error field in the observations has only a small effect on the pressure fields (Fig. 12a), especially in the upper layer. The transports are more affected by the errors (Fig. 12b). Figures 12c–d show that the assimilation of observations from the Topex/Poseidon satellite is less affected by the noise. The error in the position of the axis of the Gulf Stream is shown in Table 2. The error is not very sensitive to the noise in the observations.

The results from the 1-yr assimilation show that as for cases 5 and 6 the asymptotic values have been reached at the end of the 6-week period.

The standard errors for the pressures, the transports and the axis error are of the same magnitude as the results with no errors in the observations.

4. Summary

Assimilation of sea surface height observations has been investigated using a two-layer primitive equation model of the Gulf Stream region. In the first set of experiments complete fields of simulated sea surface height observations were used. The results from these experiments showed the importance of updating not only the upper-layer variables of the numerical model, but also the importance of transferring the altimeter information to the lower layer. The statistical inference technique of Hurlburt et al. (1990) used in an updating mode in this paper clearly enhanced the performance of the assimilation. The combination of the statistical inference technique and the dynamics of the model resulted in a rapid convergence of the assimilation. It was also shown that it is important to update the velocity field. Experiments where only the pressure fields were updated resulted in a divergence of the assimilation.

Experiments with observations sampled along two sets of simulated satellite altimeter tracks were also discussed. A 17-day repeat cycle along Geosat-ERM tracks and a 10-day repeat cycle along Topex/Poseidon tracks were sampled. Both satellites orbits yield about the same level of global rms error after 6 weeks of assimilation. Holland and Malanotte-Rizzoli (1989) and Verron (1990) reported similar results using a QG model in their assimilation studies. Holland and Malanotte-Rizzoli (1989) extracted observations along two simulated satellite tracks with repeat periods of 10 and 20 days. The experiments showed no significant difference between the two satellites in terms of global rms. Similarly, Verron (1990) studied the effect of different orbital periods. He flew four simulated satellites over his model domain. The satellites had repeat periods of 3, 10, 17, and 29 days. His results showed that the 10- and 17-day periods gave the best convergence.

The lack of large differences in global rms error for the two satellites do not imply that both satellites give equal results. The space scales of the errors from the two satellites are different. The slow temporal sampling of the Geosat-ERM results in large errors in areas where there are rapid changes in the Gulf Stream. The Topex/Poseidon low spatial resolution results in an error field with larger spatial scales covering most of the area.

One should be careful about drawing broad conclusions from these experiments. During the period of assimilation, the number of rings separating from the Gulf Stream was limited. In reality the Gulf Stream is more active than the model showed during the assimilation. This could affect the assimilation of satellite observations from a 10 day or 17 day repeat period.

The question of how much added information two satellites would give to the assimilation was also addressed. The experiments performed showed that for satellites in Geosat-ERM orbits the best results were obtained if both satellites were flying in the same orbit offset in time by half the orbital period. In the Topex/Poseidon case the best results were obtained if the two satellites were offset in space by half the distance between the tracks and offset in time by half the orbital period. The results show that there is up to a 40% reduction in the rms error if two satellites are used. The error in the position of the Gulf Stream showed a similar decrease with the additional satellites. In the Geo-

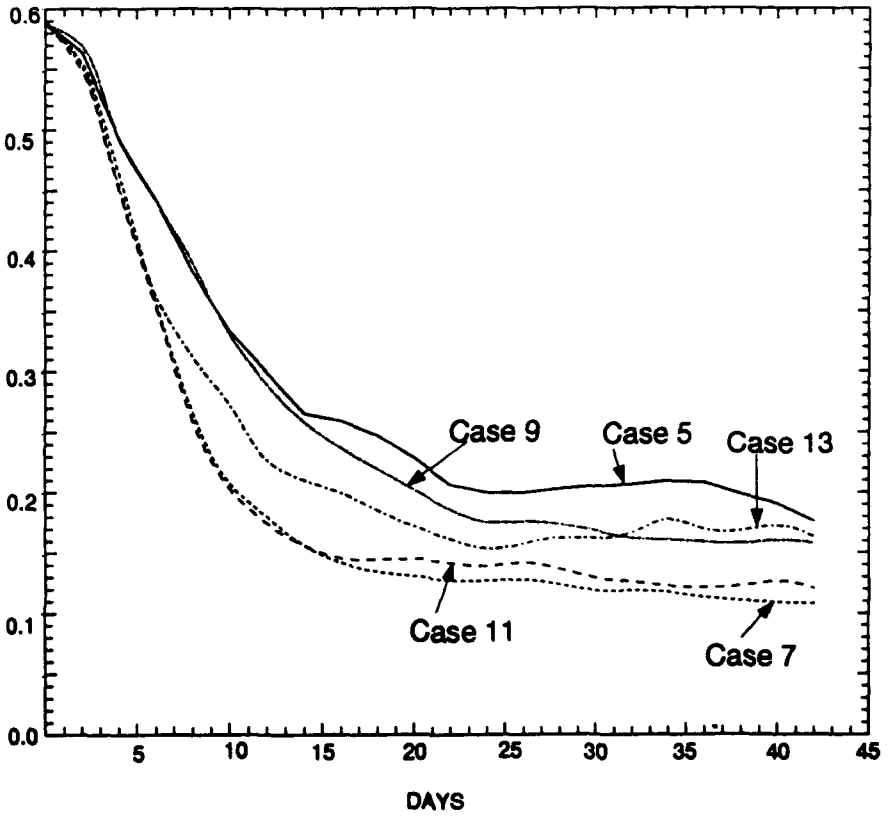
a
0.6
0.5
0.4
0.3
0.2
0.1
0.0
Case 9
Case 5
Case 13
Case 11
Case 7
5
10
15
20
25
30
35
40
45
DAYS

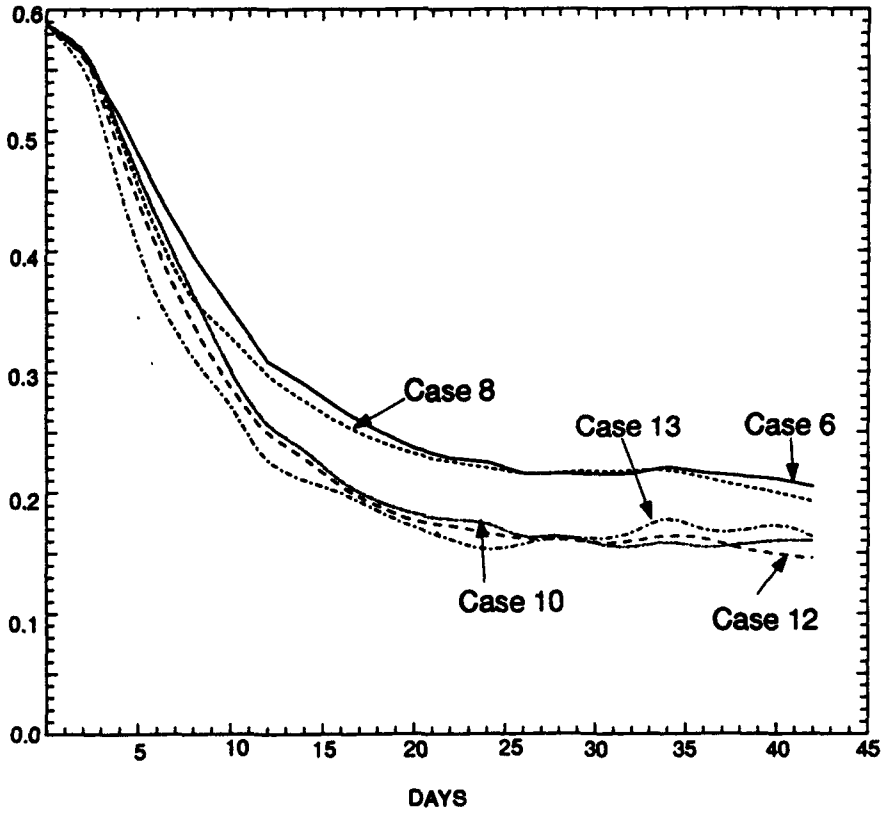
b
0.6
0.5
0.4
0.3
0.2
0.1
0.0
Case 8
Case 13
Case 6
Case 10
Case 12
5
10
15
20
25
30
35
40
45
DAYS

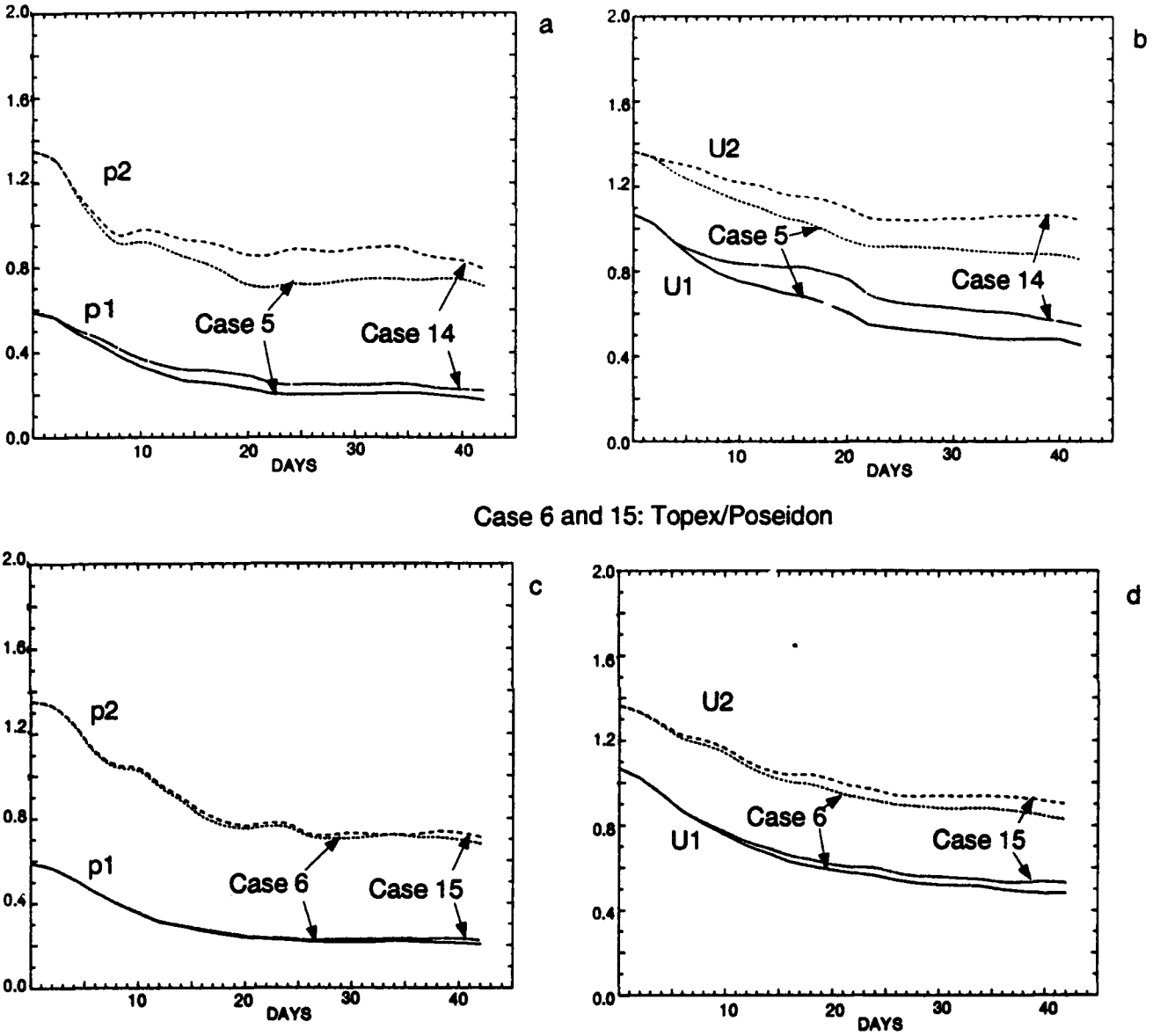

FIG. 12. The time evolution of the global rms error for the pressure updating the model along Geosat-ERM and Topex/Poseidon tracks adding a correlated error field with decorrelation scale of approximately 200 km and an rms error of 5 cm (cases 14 and 15). The experiment with noise-free observations is also shown (cases 5 and 6). The error is scaled by the variance of the observed field. (a) The pressure for Geosat-ERM, (b) the U transport for Geosat-ERM, (c) the pressure for Topex/Poseidon, and (d) the U transport for Topex/Poseidon.

sat-ERM case the error dropped from 27 km to 15 km, while in the Topex/Poseidon case the error decreased from 27 km to 20 km. The combination of one Geosat-ERM and one Topex/Poseidon satellite gave results that were better than just one satellite but not as good as the best results using two satellites of the same type.

FIG. 11. The time evolution of the global rms error for the upper-layer pressure updating the model along Geosat-ERM or Topex/Poseidon tracks. Four curves are shown for the pressure. Case 5 (Geosat-ERM) and case 6 (Topex/Poseidon) are the results with only one satellite. Cases 7 (Geosat-ERM) and 8 (Topex/Poseidon) are the results from the two satellites flying in the same orbit but offset in time by 8.5 days and 5 days, respectively. Cases 9 (Geosat-ERM) and 10 (Topex/Poseidon) show the results when the satellite orbits are offset in space, while cases 11 (Geosat-ERM) and 12 (Topex/Poseidon) are the results with the satellites in offset orbits and offset in time by 8.5 and 5 days. Case 13 shows the results using one Geosat-ERM and one Topex/Poseidon satellite. The error is scaled by the variance of the true ocean field. (a) Upper-layer pressure for Geosat-ERM satellites and (b) upper-layer pressure for Topex/Poseidon satellites.

Combining Geosat-ERM and Topex/Poseidon tracks yielded an axis error of approximately 24 km.

The experiments where white noise errors were added to the observations along satellite tracks, showed that the assimilation was not very sensitive to errors in the observations. Adding an error field with an rms of 5 cm and 10 cm to the "observations" had only a small effect on the assimilation. A correlated error field with a decorrelation scale of approximately 200 km and an rms error of 5 cm was also used. The results showed the Geosat-ERM satellite to be more sensitive to the errors than the Topex/Poseidon. This is due to the higher spatial resolution of the Geosat-ERM mission.

Acknowledgments. This work is a contribution to the 6.2 program Data Assimilation and Rapid Transition (DART) sponsored by the Office of Navy Technology, Navy Ocean Modeling Program under program element 0602435N. Many people have contributed to this project. The authors would like to thank Donna Blake, Mike Carnes, Harley Hurlburt, Jim Mitchell, and Gary Ransford. We would like to thank Warren White for making his assimilation routines available to us and Geraldine Gardiner for the use of the software calculating the axis error. The numerical simulations were performed on the Primary Oceanographic Prediction System Cray Y-MP 8/8128 at the U.S. Naval Oceanographic Office.

REFERENCES

Anthes, R. A., 1974: Data assimilation and initialization of hurricane prediction models. *J. Atmos. Sci.*, **31**, 702–718.

Bennett, A. F., and P. C. McIntosh, 1982: Open ocean modelling as an inverse problem: Tidal theory. *J. Phys. Oceanogr.*, **12**, 1004–1018.

——, and W. P. Budgell, 1987: Ocean data assimilation and the Kalman filter: Spatial regularity. *J. Phys. Oceanogr.*, **17**, 1583–1601.

——, and ——, 1989: The Kalman smoother for a linear quasigeostrophic model of ocean circulation. *Dyn. Atmos. Oceans*, **13**, 219–267.

——, and M. A. Thorburn, 1992: The Kalman smoother for a linear quasigeostrophic model of ocean circulation. *J. Phys. Oceanogr.*, **22**, 213–230.

Born, G. H., J. L. Mitchell, and G. A. Heyler, 1987: Geosat-ERM mission design. *J. Astronaut. Sci.*, **35**(2), 119–134.

Fox, D. N., M. R. Carnes, and J. L. Mitchell, 1992a: Characterizing major frontal systems: A nowcast/forecast system for the Northwest Atlantic. *Oceanography*, **5**, 49–54.

——, ——, and ——, 1992b: Circulation model experiments of the Gulf Stream using satellite derived fields. Naval Research Laboratory formal report NRL/FR/7323-92-9412.

Ghil, M., and P. Malanotte-Rizzoli, 1991: Data assimilation in meteorology and oceanography. Vol. 33, *Advances in Geophysics*, Academic Press, 141–266.

Haines, K., 1991: A direct method of assimilating sea surface height data into ocean models with adjustments to the deep circulation. *J. Phys. Oceanogr.*, **21**, 843–868.

Holland, W. R., and P. Malanotte-Rizzoli, 1989: Assimilation of altimeter data into an ocean circulation model; space versus time resolution studies. *J. Phys. Oceanogr.*, **19**, 1507–1534.

Hurlburt, H. E., 1986: Dynamic transfer of simulated altimeter data into subsurface information by a numerical ocean model. *J. Geophys. Res.*, **91**, 2372–2400.

——, and J. D. Thompson, 1980: A numerical study of Loop Current intrusions and eddy shedding. *J. Phys. Oceanogr.*, **10**, 1611–1651.

——, D. N. Fox, and E. J. Metzger, 1990: Statistical inference of weakly-correlated subthermocline fields from satellite altimeter data. *J. Geophys. Res.*, **95**, 11 375–11 409.

Kalman, R. E., 1960: A new approach to linear filtering and prediction problems. *J. Basic Eng. (Trans. ASME)*, **82D**, 35–45.

——, and R. S. Bucy, 1961: New results in linear filtering and prediction theory. *J. Basic Eng. (Trans. ASME)*, **83D**, 95–108.

Kistler, R. E., 1974: A study of data assimilation techniques in an autobarotropic, primitive equation, channel model. M.S. thesis, Department of Meteorology, The Pennsylvania State University, 84 pp.

Malanotte-Rizzoli, P., and W. R. Holland, 1986: Data constraints applied to models of the ocean general circulation. Part I: The steady case. *J. Phys. Oceanogr.*, **16**, 1665–1682.

——, and ——, 1988: Data constraints applied to models of the ocean general circulation. Part II: The transient, eddy-resolving case. *J. Phys. Oceanogr.*, **18**, 1093–1107.

——, R. E. Young, and D. B. Haidvogel, 1989: Initialization and data assimilation experiments with a primitive equation model. *Dyn. Atmos. Oceans*, **13**, 349–378.

Mellor, G. L., and T. Ezer, 1991: A Gulf Stream model and an altimetry assimilation scheme. *J. Geophys. Res.*, **96**, 8779–8795.

Miller, R. N., 1986: Toward the application of the Kalman filter to regional open ocean modelling. *J. Phys. Oceanogr.*, **16**, 72–86.

——, 1990: Tropical data assimilation experiments with simulated data: The impact of the tropical ocean and the global atmosphere thermal array for the ocean. *J. Geophys. Res.*, **95**, 11 461–11 482.

——, and M. A. Cane, 1989: A Kalman filter analysis of sea level height in the tropical Pacific. *J. Phys. Oceanogr.*, **19**, 773–790.

Orlanski, I., 1976: A simple boundary condition for unbounded hyperbolic flows. *J. Comput. Phys.*, **21**, 251–269.

Provost, C., and R. Salmon, 1986: A variational method for inverting hydrographic data. *J. Mar. Res.*, **44**, 1–34.

Sheinbaum, J., and D. L. T. Anderson, 1990a: Variational assimilation of XBT data. Part I. *J. Phys. Oceanogr.*, **20**, 672–688.

——, and ——, 1990b: Variational assimilation of XBT data. Part II: Sensitivity studies and use of smoothing constraints. *J. Phys. Oceanogr.*, **20**, 689–704.

Smedstad, O. M., and J. J. O'Brien, 1991: Variational data assimilation and parameter estimation in an equatorial Pacific Ocean model. *Progress in Oceanography*, Vol. 26, Pergamon, 179–241.

Thacker, W. C., 1986: Relationships between statistical and deterministic methods of data assimilation. *Variational Methods in the Geosciences*, Y. K. Sasaki, Ed., Amsterdam, 173–179.

——, 1989: The role of the Hessian matrix in fitting models to measurements. *J. Geophys. Res.*, **94**, 6177–6196.

——, and R. B. Long, 1988: Fitting dynamics to data. *J. Geophys. Res.*, **93**, 1227–1240.

Thompson, J. D., 1986: Altimeter data and geoid error in mesoscale ocean prediction: Some results from a primitive equation model. *J. Geophys. Res.*, **91**, 2401–2417.

——, and W. J. Schmitz, 1989: A limited-area model of the Gulf Stream: Design, initial experiments, and model-data intercomparison. *J. Phys. Oceanogr.*, **19**, 791–814.

Verron, J., 1990: Altimeter data assimilation into an ocean circulation model: Sensitivity to orbital parameters. *J. Geophys. Res.*, **95**, 11 443–11 459.

——, 1992: Nudging satellite altimeter data into quasi-geostrophic ocean models. *J. Geophys. Res.*, **97**, 7479–7491.

Wallcraft, A. J., 1991: The Navy Layered Ocean Model users guide. NOARL Report 35, Stennis Space Center, MS, 21 pp.

Watts, D. R., 1983: Gulf Stream variability. *Eddies in Marine Science*, A. R. Robinson, Ed., Springer Verlag, 114–143.

White, W. B., C. K. Tai, and W. R. Holland, 1990a: Continuous assimilation of simulated Geosat altimetric sea level into an eddy resolving numerical model. Part 1: Sea level differences. *J. Geophys. Res.*, **95**, 3219–3234.

——, ——, and ——, 1990b: Continuous assimilation of simulated Geosat altimetric sea level into an eddy resolving numerical model. Part 2: Referenced sea level differences. *J. Geophys. Res.*, **95**, 3235–3252.

——, ——, and ——, 1990c: Continuous assimilation of Geosat altimetric sea level observations into a numerical synoptic ocean model of the California Current. *J. Geophys. Res.*, **95**, 3127–3148.